THE ASTROPHYSICAL JOURNAL, 429:380–384, 1994 July 1

THE RADIO SOURCE AROUND η CARINAE

S. M. WHITE,[1] R. A. DUNCAN,[2] J. LIM,[3] G. J. NELSON,[4] S. A. DRAKE,[5] AND M. R. KUNDU[1]

Received 1993 October 13; accepted 1994 January 3

ABSTRACT

We present high spatial resolution radio observations of the peculiar southern star η Carinae, made with the Australia Telescope. The images, at 8 and 9 GHz with a resolution of 1.″0, show a source of dimension 10″ and total flux of 0.7 Jy dominated by a strong central peak. The radio emission is unpolarized and offers no support to models which invoke degenerate stars or more exotic objects within the core of η Car. In these data we find no evidence for more than one energy source in the core with arcsecond separations as some infrared observations have suggested. Several levels of structure are evident in the radio image, which shows symmetry on the larger scales. Conventional formulae for stellar wind radio sources give a mass loss rate of order $3 \times 10^{-4}\ M_{\odot}\ \mathrm{yr}^{-1}$ based on the radio flux in the central peak, which yields a wind momentum flux of order 20% of the momentum flux available from the star's radiation field. The radio emission at these frequencies is consistent with thermal emission from gas flowing away from a "luminous blue variable" star (LBV). η Car is probably the brightest thermal stellar wind radio source in the sky.

Subject headings: circumstellar matter — radio continuum: stars — stars: individual (η Carinae) — supergiants

1. INTRODUCTION

η Carinae is one of the most famous and intriguing stars in the Galaxy. In the 1830s it underwent an outburst which converted it from a second magnitude star (fourth magnitude in 1677) to the second brightest star in the sky (mag = −1); since then, its visual brightness has declined to seventh magnitude. The visual dimming since the 1840s does not mean that the bolometric luminosity of the star has dropped accordingly: in the 1960s it was found to be the brightest (extra–solar system) infrared source in the sky at 10 and 20 μm, and the bolometric luminosity presently is estimated to be similar to the visual luminosity during the outburst, when most of the radiation was probably in the visual region of the spectrum. The peculiarities of this star have led to many speculations regarding its nature. It has been variously explained as a massive pre–main-sequence star (Gratton 1963), a slow supernova (Thackeray 1956; Ostriker & Gunn 1971), a single massive OB star (Davidson 1971), an accretion-powered source (Bath 1979), a binary system of massive stars (Warren-Smith et al. 1979), a possibly binary F-type hypergiant (Viotti et al. 1989), a four-star system (Weigelt & Ebersberger 1986), and, most recently, a point source of cosmic rays embedded in dust (Borgwald & Friedlander 1993).

The most widely accepted view is that it is a member of the class of stars known as "luminous blue variables" (LBVs), which are characterized by large but variable luminosities, hot colors, and rapid and often unsteady mass loss (Conti 1984; Humphreys 1989). They are thought to be evolved massive stars in a short-lived state prior to becoming Wolf-Rayet stars: during this state they shed their outer layers, through some unknown mechanism which probably involves an instability due to radiation pressure. The outburst in the 1830s is thought to have been such an event, in which η Car ejected up to 3 $M_{\odot}$ of material rich in heavy elements, and dust formed from this material now absorbs the bulk of the stellar luminosity of $10^{6.5}$ $L_{\odot}$ which is radiated by the star at optical and ultraviolet wavelengths. The heated dust reradiates the luminosity in the infrared. There are several tracers of mass loss in the immediate environment of the star: the "core," the very bright but non-stellar central region of dimension several arcseconds associated with the current wind; the "Homunculus," a high surface brightness nebulosity of dimension 12″ × 17″ resulting from the ejection in the 1830s; and an outer shell which comprises a number of features out to a distance of about 25″, mostly resulting from even earlier ejections (Walborn 1976; Walborn, Blanco, & Thackeray 1978). Recent high-resolution (0.″2) observations of η Car with the Wide Field Camera on the *Hubble Space Telescope* (*HST*) resolve one feature in the outer shell into a jetlike feature crossed by short bars, resembling the rungs of a ladder (Hester et al. 1991).

Despite the enormous number of papers published on η Car, it remains poorly understood. Nearly every new paper on the subject suggests a new interpretation for the distribution of material around the star. One of the few wavelength ranges in which it has received relatively little attention is that of radio, due to the lack of telescopes in the southern hemisphere capable of the arcsecond resolution necessary to adequately resolve this source. The best radio image of the region to date was obtained by Retallack (1983) using the Fluers synthesis telescope at 1.4 GHz. This image had spatial resolution of 50″; in it, η Car appears as a compact source of 0.9 ± 0.3 Jy. Jones (1985) observed η Car at 843 MHz with the Molonglo Observatory Synthesis Telescope: this observation had a beam of 49″ × 43″, and a flux of 1.1 ± 0.3 Jy was measured.

With the commissioning of the Australia Telescope (AT) in 1988, arcsecond-resolution imaging of radio sources in the southern sky is now possible. Radio observations of this source are clearly important for their ability to penetrate the dust shell

[1] Department of Astronomy, University of Maryland, College Park, MD 20742.
[2] Australia Telescope National Facility, P.O. Box 76, Epping NSW 2121, Australia.
[3] Solar Astronomy 264–33, Caltech, Pasadena, CA 91125.
[4] ATNF/Paul Wild Observatory, P.O. Box 94, Narrabri NSW 2390, Australia.
[5] Laboratory for High Energy Astrophysics, NASA/GSFC, Greenbelt, MD 20771.

surrounding the star and reveal the ionized gas below it; they can also study the interaction of the expanding ejecta with the surrounding medium, which may be analogous to that of a supernova remnant. Detection of polarized jets could confirm the role of magnetic fields in determining the morphology of the nebula, as suggested by Hester et al. (1991), while a polarized core would imply the presence of a compact object. Here we present images of the radio source around η Car at the best achievable resolution of the AT in its current configuration (1.″0) and argue that they are consistent with thermal emission from an LBV.

2. OBSERVATIONS AND ANALYSIS

Two observations of η Carinae were carried out with the AT in 1992. The AT consists of six 22 m antennas (five of which are moveable) in an east-west array, with a maximum baseline of 6 km. Since the Fleurs image of the Carina region suggested that the radio source around η Car might be as large as 40″ and also that there would be a lot of other structure within the field of view at this scale size associated with the Carina nebula, we carried out one observation with the five movable antennas in a compact configuration (0.375 km, 1992 April 29) in order to map large structures, and a second observation in a much wider configuration (6.0 A, 1992 June 28) which was not sensitive to large structures.

In addition to excellent low noise receivers, the AT offers the advantage of a large receiving bandwidth. In a standard continuum observation, two frequencies, each of bandwidth 128 MHz and split into 32 channels, are recorded simultaneously. On April 29 the frequencies we observed were 8256 MHz and 9024 MHz, while on June 28 they were 8128 MHz and 9024 MHz. The map made from the April 29 data, sensitive to large spatial scales, shows an 0.7 Jy source at the position of η Car, unresolved at the resolution of 13″, together with extended nebular emission to the northwest. We will not discuss these data further here. The June 28 data, taken in a configuration which has baselines almost uniformly spaced from 350 to 6000 m, proves to be almost ideal for the study of the η Car radio source since the nebular emission is resolved out. Wide-field maps made from this data show no other sources in the field of view; the two shortest baselines do show evidence of the larger structures present but are nonetheless dominated by the flux from η Car. The final 9 GHz map is shown in Figure 1. The peak flux is 0.17 Jy beam^{-1} with a map rms of 0.00012 Jy beam^{-1}, for a beam size of 1.″0 × 0.″92 (uniform weighting). The 8 GHz image has a beam 10% larger, but a peak flux which is the same as that of the 9 GHz map (0.17 Jy). The 8 GHz image is virtually identical in appearance to the 9 GHz image in Figure 1. It has slightly more total flux in the η Car radio source (0.66 Jy, compared with 0.64 Jy at 9 GHz), but this may be attributed to the fact that there is not enough information in the shortest baselines of this observation at either frequency to completely recover all the flux of the source. We are therefore confident that Figure 1 provides a good representation of all the important features of the radio source around η Carinae, except possibly in the low-level flux associated with the most extended emission.

3. THE RADIO PROPERTIES OF η CARINAE

3.1. *Radio Morphology*

There are a number of different structures revealed in Figure 1. First, the radio source shows a strong central peak. The position of the radio peak differs from the star's optical position by 0.″2 in R.A. and 0.″6 in decl., but unfortunately the AT's baseline solutions were not applied correctly during the period including this observation, which leads to an uncertainty in our astrometry of order 1″ (M. Wieringa & N. Killeen, private communication). Therefore we assume that the radio peak is in fact coincident with the optical peak. The brightness temperature T_b corresponding to the peak flux is 3000 K. Cuts through the central peak at 45° and 135°, approximately along the major and minor axes of the Homunculus nebula, give a FWHM of 1.″6 in both directions. At the distance of η Carinae (2.5 kps), 1″ corresponds to a dimension of 0.012 kpc.

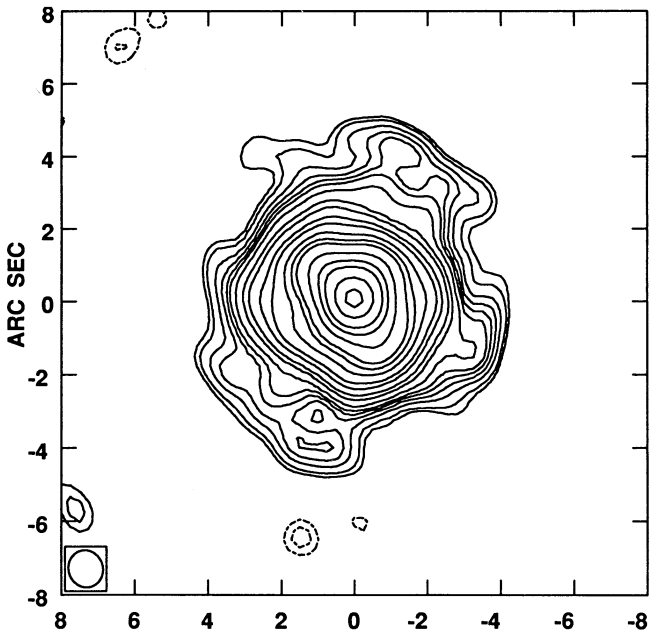

FIG. 1.—A contour plot of the AT 9.0 GHz image of η Carinae. Contours are at multiples −4, −3, 3, 4, 6, 8, 10, 12, 16, 24, 32, 48, 64, 98, 128, 160, 256, 384, 512, 768, and 1024 of 0.15 beam^{-1}, with a beam size of 1.″0 × 0.″92 (clean beam shown at bottom left).

To compare the radio image with the distribution of gas seen in optical data we have extracted an *HST* Planetary Camera observation in the [N II] λ6584 line from the public *HST* data archive and deconvolved the image for the effects of the spherical aberration of the *HST* mirror. This line represents relatively cool gas. In Figure 2 we have overlaid contours of the radio image, at logarithmically spaced intervals, on a gray-scale representation of the *HST* image, which is also scaled logarithmically to show as much dynamic range as possible. Since we do not have absolute astrometry for the radio image, we have aligned the images assuming that the strong peaks in each are coincident. The dark streak and narrow line in the *HST* image running from upper left to lower right are artefacts due to saturation of the central source on the CCD chip.

Just beyond the central peak, two asymmetries are evident in the radio map (Fig. 1). Ridges extend away from the central peak along NE–SW axes, out to a radius of ∼2.″5; further ridges extend along SE–NW axes out to a radius of ∼1.″5. These axes are loosely, but not closely, aligned with the symmetry axes of the optical Homunculus nebula. Beyond these ridges is a box-shaped structure with relatively sharp edges, of dimension 6″ (NE–SW) × 5″ (SE–NW), which is also evident in the IR images (discussed further below). The axes of this structure agree with the ridges discussed above, and with the axes of the Homunculus. However, the major axis of the radio "box"

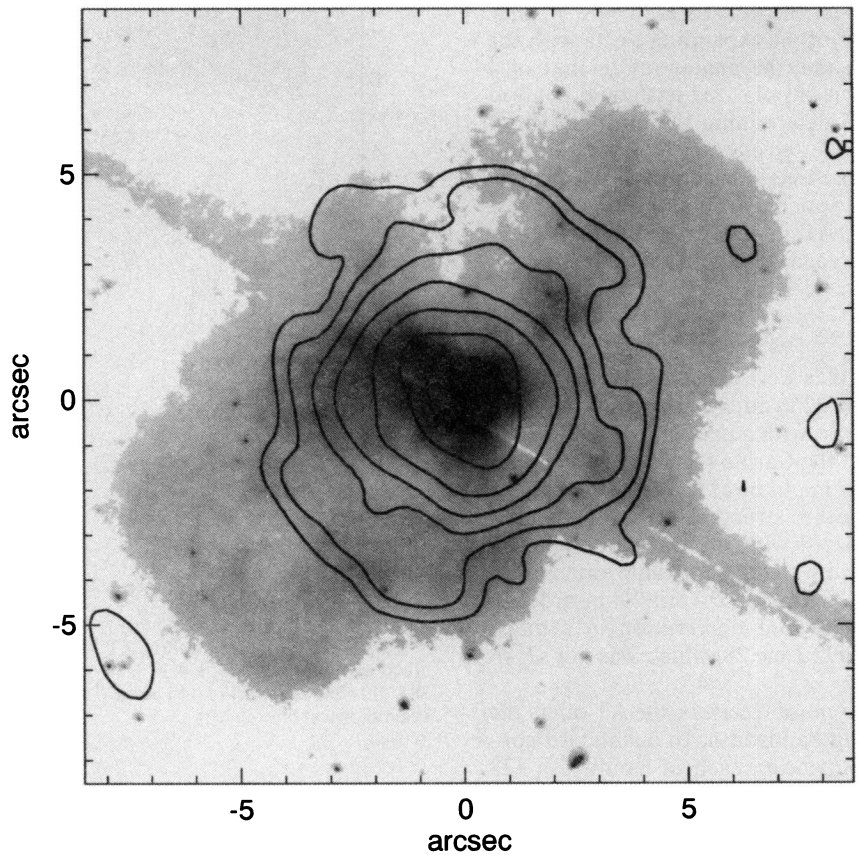

FIG. 2.—Radio contours overlaid on an *HST* Planetary Camera [N II] λ6584 image of η Carinae. The *HST* image is displayed with a logarithmic representation of the intensity, and the radio contours are also logarithmically spaced, at brightness temperatures of 5, 13, 32, 79, 200, 501, 1260, and 3162 K. The streak and bright line in the *HST* image running from upper left to lower right are artefacts due to saturation of the central peak.

is orthogonal to the major axis of the Homunculus. The flux level characteristic of the box is around 0.01 Jy beam^{-1}, or a brightness temperature of 170 K.

Extending beyond the sharp drop at the edge of this box are two "handles," to the SE and NW. These correspond roughly to the directions of the lobes (the "head" and "feet") of the Homunculus. In the 9 GHz map these handles extend out to 5″ from the central peak; in the 8 GHz map they extend slightly further out. A similar but less pronounced projection may be seen to the SW of the box feature: this too is present in the 8 GHz map. The flux level in these features is ∼0.0015 Jy beam^{-1}, or $T_b \sim 25$ K. It is possible that these features are artefacts of the limited *uv* coverage provided by six antennas.

The overall dimension of the radio source around η Carinae in Figure 1 is 10″ × 8″, with the major axis approximately in the direction of the major axis of the Homunculus. This is about half the dimension of the optical Homunculus in the same direction. As noted earlier, the maximum dimension for the radio source obtained here may be limited by the shortest baseline present in the observation.

3.2. *Polarization*

We have made maps of η Carinae in Stokes *Q*, *U*, and *V*. In each of the resulting maps the rms was ∼0.000075 Jy beam^{-1}, or less than 0.05% of the peak flux in the Stokes *I* map. There is no evidence for any flux above the 4 σ level in the Stokes *Q* and *U* maps (the linearly polarized flux). There is a 6 σ source in the Stokes *V* (circularly polarized flux) map at the location of the peak in the total intensity map, but since this is at a level of less than 0.3% of the total intensity peak and as errors in the reconstruction of circular polarization from the received linear polarizations are expected to be at this level, we do not regard it as significant.

The 8 and 9 GHz maps have the same peak flux although the beam is larger at 8 GHz, indicating that the central core has a spectrum flat or falling to lower frequencies, whereas optically thin nonthermal emission would be expected to rise toward lower frequencies. This result together with the absence of any linearly polarized emission makes it unlikely that any significant fraction of the flux in the core at 8–9 GHz is due to synchrotron emission in an ordered magnetic field. However, we cannot rule out the possibility that there is linear polarization in the intrinsic emission which is destroyed by differential Faraday rotation as the radiation propagates through the dense ionized medium around the star.

3.3. *Comparison with Infrared Images*

The extended radio emission corresponds well to infrared (IR) images taken at similar resolution. A box-shaped feature of size similar to the "box" in Figure 1 was seen by Hyland et al. (1979), Hackwell, Gehrz, & Grasdalen (1986), Russell et al. (1987), and Allen (1989), typically at wavelengths of order 10 μm. However, a number of these studies have found multiple sources within the inner few arcseconds of the region: typically they have found two sources of nearly equal intensity with a separation of 1″, at a position angle of about 55° (measured east from north; Hyland et al. 1979; Mitchell et al. 1983; Hackwell et al. 1986). This led to the suggestion that there might be

two energy sources in the Homunculus nebula. The alignment of the "second source" corresponds remarkably well with the ridge to the NE in the radio map. However, Allen (1989) presents high-resolution images at 1.2, 2.2, 3.8, and 4.8 μm which all show the core to be dominated by a single bright peak, but also show a ridge to the NE. Allen (1989) argues that previous detections of a double structure in the core at this wavelength were incorrect. Our radio observations would have resolved two sources of similar brightness 1″ apart, but we see no evidence for this. We therefore argue that at an arcsecond scale there is only one source. Speckle observations sensitive to even smaller spatial scales have further complicated the picture: Weigelt & Ebersberger (1986) and Hofmann & Weigelt (1988) interpret their near-IR speckle observations as indicating a strong central peak together with three other sources within 0.″2, approximately an order of magnitude fainter than the peak. Our radio data are not sensitive to these small scales.

3.4. *Comparison with High-Resolution HST Optical Image*

The *HST* image displayed in Figure 2 was made with a very short integration, optimal for revealing the features close to the central region, and it shows a bright knot $\sim 1''$ to the northeast of the peak, underlying the radio and Allen's (1989) IR "ridge." We suggest that this knot may have been the cause of the "second source" seen in earlier IR observations, but that its true intensity (in radio and IR) is well below that of the star. This image reveals the lumpy nature of the distribution of gas close to the star. It seems unlikely that the radiation emerging at the photosphere of the star is not spherically symmetric, so the knots must arise due to processes in the outflowing wind, perhaps as part of the process of transferring momentum from the radiation field to the matter.

Notwithstanding the inhomogeneities, both the radio and optical images show a large degree of symmetry on larger scales. However, they have different symmetry axes, as seen in Figure 2. The major axis of the optical Homunculus nebula is at a position angle of 132° on the sky, whereas the radio nebula has a symmetry axis (at the largest scales) at about 145°. This suggests different symmetry axes for the eruption of the 1830s and subsequent events. At present we have no explanation for this.

4. THE WIND OF η CARINAE

We assume that the strong central peak of the radio source is due to thermal emission from the stellar wind. It is however difficult to separate the contribution of the wind from the contribution of the rest of the nebula. Fits to the central peak alone give a total flux of 0.29 ± 0.006 Jy at both 8.1 and 9.0 GHz, with deconvolved sizes of $1''.74 \times 1''.36$ at PA 26° at 8.1 GHz, and $1''.49 \times 1''.28$ at PA 29° at 9.0 GHz. The peak flux of the fit to the core component is 0.14 ± 0.002 Jy at each frequency. The fact that the radio peak has the same flux per beam at both 8.1 and 9.0 GHz means that the temperature is identical at the two frequencies (~ 3000 K), which is consistent with an optically thick wind source. In most stellar wind sources there is no significant radio emission from above the optically thick surface, since density falls off so rapidly, but in the case of η Car there is clearly material present not associated with a constant spherically symmetric wind. There is no unique fit to the wind flux in these data; we will adopt a radio flux for the wind component of 0.2 ± 0.1 Jy. The stellar wind velocity is believed to be $v_W = 500$ km s^{-1} (e.g., Hillier & Allen 1992), and at a distance of 2.5 kpc the derived mass-loss rate in the current stellar wind is

$$\dot{M} = 3(\pm 1) \times 10^{-4} \frac{v_W}{500 \text{ km s}^{-1}} M_\odot \text{ yr}^{-1},$$

with the usual assumptions of constant temperature, full ionization, and spherical symmetry. This result is consistent with the upper limits of $10^{-2.4}\ M_\odot$ yr^{-1} obtained by Davidson et al. (1986) from the infrared and hot inner dust properties, and $10^{-3}\ M_\odot$ yr^{-1} by Davidson (1987) from the need for compatibility between the observed radiation temperature and the wind opacity. Van Genderen & Thé (1984) estimated a value of $1\text{–}2 \times 10^{-4}\ M_\odot$ yr^{-1} from several arguments. The oft-quoted estimate of $0.075\ M_\odot$ yr^{-1} by Andriesse, Donn, & Viotti (1978) is not consistent with our observation. This is important because it implies that the mechanical power available in the wind for heating is much less than the value derived by Andriesse et al. (1978). That value was used by Viotti et al. (1989) for their model in which η Car has a cool photosphere ($< 10^4$ K) and its wind is heated by conversion of the energy associated with bulk motion into heat. According to the numbers given above, the mechanical energy associated with the wind is only about $10^4\ L_\odot$, or more than two orders of magnitude smaller than derived by Andriesse et al. (1978). A corollary of the estimate obtained here is that the mass lost by the star through its wind since the 1860s ($\sim 0.05\ M_\odot$) is much less than the amount of mass ejected during the outburst of 1830–1860 ($\sim 1\ M_\odot$; cf. Davidson 1989).

To put the wind properties into perspective, we note that at 0.″5 from the star (0.006 pc, the half-power point of the radio image) the wind density is 4×10^3 cm^{-3}, and it takes 10 yr for the wind to propagate from the stellar surface to this height. Since the stellar radiation field is believed to drive the winds of hot stars, in principle the momentum flux of the wind of η Car should not exceed the radiation momentum flux at the photosphere. The wind momentum flux is $\dot{M} v_W = 1 \times 10^{29}$ g cm s^{-2}; the radiation momentum flux, based on the current bolometric luminosity of the star, is $L_*/c = 6 \times 10^{29}$ g cm s^{-2}. Thus the radiation field has enough momentum to drive the wind by a comfortable margin.

5. DISCUSSION

The radio image of η Carinae resembles an ultracompact H II region (UC H II R; Churchwell 1990) in its size, brightness temperature, and to some extent morphology, UC H II Rs are small, photoionized nebulae with high electron density and large emission measure. They are believed to form around newly born hot massive stars as the ultraviolet photons from the young star ionize the dense coccoon of material in the molecular cloud from which it formed. Typically, they are strong compact radio sources and bright infrared sources. The stars themselves are not usually visible. But there is one major difference between η Car and an UC H II R. In the case of UC H II Rs, all the dust and gas near the star is assumed to be remnants of the natal coccoon in which the star was born, with roughly uniform density everywhere. However, we assume that η Car is a mature massive star which has been driving strong outflows into its environment for several million years, and these outflows will have dispelled all material from the natal cloud. All the material we see close to the star has come from the star itself, and should be strongly centrally concentrated.

In particular, the dust responsible for all the IR emission seen close to the star must form out of the wind and can do so only when the wind has cooled sufficiently from its photo-

spheric temperature of around 30,000 K (see Davidson et al. 1986). Andriesse et al. (1978) also argue that the wind cools significantly as it propagates away from the star, unlike conventional hot-star models in which the wind temperature is maintained at the effective temperature of the star by the radiation field. The actual temperature at which dust will form depends on the grain composition: the dust around η Car is thought to be largely silicate grains, which could form at about 3000 K if the gas is sufficiently dense. Coincidentally, 3000 K is the peak brightness temperature in the radio maps, if the central peak is resolved. However, Andriesse et al. (1978) have made the point that the partial pressures of the constituents of silicate grains in η Car's wind may not be high enough for silicate dust to form at a resonable height. They derive a required density of at least 10^{15} cm^{-3}, which would make dust formation anywhere unlikely. However, the basic point that dust formation in a spherically symmetric wind is inefficient seems valid and suggests instead that dust forms preferentially in dense clumps of gas flowing out from the star, consistent with the "knottiness" or inhomogeneity of the material close to the star for which evidence is found at all wavelengths, e.g., Viotti et al. (1989) find a wide range of ionization states in UV lines from the wind, implying that the wind is characterized by components with a range of temperatures, and Davidson et al. (1986) argue that the inner dust shell cannot be opaque to UV because much of the infrared luminosity arises in cooler dust further than 1″ from the star, concluding that inhomogeneities must be present in the shell to make it at least partially transparent. This can also explain why there is so much radio emission from outside the optically thick surface in the stellar wind where the temperature appears to be only 3000 K. There is plenty of residual material above this surface from past ejections which has high density and can be ionized provided sufficient UV flux can pass through the inner dust shell. We assume that such material provides the optically thin, low brightness temperature radio nebula out to 5″ from the star, while the radio core is due to the present-day wind.

Since the morphological similarities between the radio and IR maps are so strong, we need to address the possibility that some of the radio emission arises from the warm dust itself. Assuming the dust to be optically thin, we expect flux spectra of f^3 and f^4 for dust emissivity laws $\epsilon \propto f$ and $\epsilon \propto f^2$, respectively. For such spectra the flux should rise by factors of 37% and 52%, respectively, between 8.1 and 9.0 GHz. Such large increases would easily have been seen in our maps, but instead the maps indicate that, e.g., the box-shaped feature in the radio map has a flux spectrum which is flat to better than 10% from 8.1 to 9.0 GHz. We conclude that it is unlikely that any significant fraction of the radio emission is produced by dust.

6. CONCLUSIONS

We have presented the first high spatial resolution radio image of the star η Carinae. It is a strong and resolved radio source with a total flux of 0.7 Jy at 9 GHz. The radio image is dominated by a strong central peak, but much of the flux is in the surrounding extended emission. Several ridges project away from the central peak. The most prominent radio ridge is to the northeast and coincides with a bright optical knot seen in an *HST* image of the star. Interpreting the radio peak as the optically thick stellar wind, we find a mass-loss rate of order $3 \times 10^{-4}\ M_\odot\ \mathrm{yr}^{-1}$; the corresponding momentum flux in the wind is then 20% of the momentum flux available in the radiation field. The radio nebula surrounding the stellar wind source is assumed to be due to photoionization of material ejected previously and requires that at least some of the stellar UV be able to penetrate the inner dust shell surrounding the star. There is no evidence for any nonthermal emission associated with the radio core. The peak brightness temperature associated with the radio source is only 3000 K.

The stellar wind takes approximately 10 yr to propagate out to the distance 0.″5 above the star which corresponds to the resolution of the radio images, and we can expect to measure variations in the wind on approximately this timescale with further radio observations. Recombination line observations to measure velocities in the outflowing gas and lower frequency observations to look for interaction between the outflowing material and the surrounding medium will be presented elsewhere.

This research has made use of the SIMBAD database, operated at CDS, Strasbourg, France. We thank the UserSupport Branch and Data Systems Operation Branch of the Space Telescope Science Institute for assistance with retrieval of archival *HST* data. This research was supported at the University of Maryland by NSF grants AST 91-14918 and 92-17891. S. W. also gratefully acknowledges the support of a US-Australia Collaborative Research grant from the National Science Foundation (administered by the National Radio Astronomy Observatory) for the completion of this work.

REFERENCES

Allen, D. A. 1989, MNRAS, 241, 195
Andriesse, C. D., Donn, B. D., & Viotti, R. 1978, MNRAS, 185, 771
Bath, G. T. 1979, Nature, 282, 274
Borgwald, J. M., & Friedlander, M. W. 1993, ApJ, 408, 230
Churchwell, E. 1990, Astron. Astrophys. Rev., 2, 79
Conti, P. S. 1984, in IAU Symp. 105, Observational Tests of Stellar Evolution Theory, ed. A. Maeder & A. Renzini (Dordrecht: Reidel), 233
Davidson, K. 1971, MNRAS, 154, 415
———. 1987, ApJ, 317, 760
———. 1989, in IAU Colloq. 113, Physics of Luminous Blue Variables, ed. K. Davidson, A. F. J. Moffat, & H. J. G. L. M. Lamers (Dordrecht: Kluwer), 101
Davidson, K., Dufour, R. J., Walborn, N. R., & Gull, T. R. 1986, ApJ, 305, 867
Gratton, L. 1963, in Star Evolution, ed. L. Gratton (New York: Academic), 297
Hackwell, J. A. Gehrz, R. D., & Grasdalen, G. L. 1986, ApJ, 311, 380
Hester, J. J., Light, R. M., Westphal, J. A., Currie, D. G., Groth, E. J., Holtzmann, J. A., Lauer, T. R., & O'Neil, E. J., Jr. 1991, AJ, 102, 654
Hillier, D. J., & Allen, D. A. 1992, A&A, 262, 153
Hofmann, K.-H., & Weigelt, G. 1986, A&A, 203, L21
Humphreys, R. M. 1989, in IAU Colloq. 113, Physics of Luminous Blue Variables, ed. K. Davidson, A. F. J. Moffatt, & H. J. G. M. Lamers (Dordrecht: Kluwer), 3
Hyland, A. R., Robinson, G., Mitchell, R. M., Thomas, J. A., & Becklin, E. E. 1983, ApJ, 233, 145
Jones, P. A. 1985, MNRAS, 216, 613
Mitchell, R. M., Robinson, G., Hyland, A. R., & Jones, T. J. 1983, ApJ, 271, 133
Ostriker, J. P., & Gunn, J. E. 1971, ApJ, 164, L95
Retallack, D. S. 1983, MNRAS, 204, 669
Russell, R. W., Lynch, D. K., Hackwell, J. A., Rudy, R. J., Rosano, G. S., & Castelaz, M. W. 1987, ApJ, 321, 937
Thackeray, A. D. 1956, Observatory, 76, 103
van Genderen, A. M., & Thé, P. S. 1984, Space Sci. Rev., 39, 317
Viotti, R., Rossi, L., Cassatella, A., Altamore, A., & Baratta, G. B. 1989, ApJS, 71, 983
Walborn, N. R. 1976, ApJ, 204, L17
Walborn, N. R., Blanco, B. M., & Thackeray, A. D. 1978, ApJ, 219, 498
Warren-Smith, R. F., Scarott, S. M., Murdin, P., & Bingham, R. G. 1979, MNRAS, 187, 761
Weigelt, G., & Ebersberger, J. 1986, A&A, 163, L5